Published in final edited form as:
J Immunol. 2013 March 15; 190(6): 2807–2817. doi:10.4049/jimmunol.1203265.

Microglia and a Functional Type I IFN Pathway are Required to Counter HSV-1-Driven Brain Lateral Ventricle Enlargement and Encephalitis[1]

Christopher D. Conrady[*], **Min Zheng**[†], **Nico van Rooijen**[¶], **Douglas A. Drevets**[§], **Derek Royer**[*], **Anthony Alleman**[#,§], and **Daniel J. J. Carr**[*,†,2]

[*]Department of Microbiology and Immunology, University of Oklahoma Health Sciences Center, Oklahoma City, OK, USA [†]Department of Ophthalmology, University of Oklahoma Health Sciences Center, Oklahoma City, OK, USA [#]Department of Radiological Sciences, University of Oklahoma Health Sciences Center, Oklahoma City, OK, USA [§]Department of Medicine, University of Oklahoma Health Sciences Center, Oklahoma City, OK, USA [¶]Department of Molecular Cell Biology and Immunology, VU Medical Center, Amsterdam, The Netherlands

Abstract

HSV-1 is the leading cause of sporadic viral encephalitis with mortality rates approaching 30% despite treatment with the antiviral drug of choice, acyclovir. Permanent neurological deficits are common in patients that survive but the mechanism leading to this pathology is poorly understood impeding clinical advancements in treatment to reduce central nervous system (CNS) morbidity. Using magnetic resonance imaging and type I IFN receptor deficient mouse chimeras, we demonstrate HSV-1 gains access to the murine brain stem and subsequently brain ependymal cells leading to enlargement of the cerebral lateral ventricle and infection of the brain parenchyma. A similar enlargement in the lateral ventricles is found in a subpopulation of herpes simplex encephalitic patients. Associated with encephalitis is an increase in CXCL1 and CXCL10 levels in the cerebral spinal fluid, TNF-α expression in the ependymal region and the influx of neutrophils of encephalitic mouse brains. Reduction in lateral ventricle enlargement using the anti-secretory factor peptide, AF-16, reduces mortality significantly in HSV-1 infected mice without any effect on expression of inflammatory mediators, infiltration of leukocytes, or changes in viral titer. Microglial cells but not infiltrating leukocytes or other resident glial cells or neurons are the principal source of resistance in the CNS during the first 5 days post infection through a TRIF-dependent, type I IFN pathway. Our results implicate lateral ventricle enlargement as a major cause of mortality in mice and speculate such an event transpires in a subpopulation of human herpes simplex virus encephalitic patients.

Introduction

HSV-1 is the leading cause of sporadic viral encephalitis, a rapidly progressive and severely debilitating disease with mortality rates approaching 70% in the untreated human patient (1). In those patients that do survive, permanent neurological deficits are not uncommon (1). During herpes simplex encephalitis (HSE)[3], patients suffer from acute psychosis, temporal

[1]This work was supported in part by NIH grant AI053108 to DJJC. Additional support includes P20 RR017703, a senior investigator award from Research to Prevent Blindness and an OUHSC Presbyterian Health Foundation Presidential Professorship award to DJJC.

[2]Corresponding author: Daniel J.J. Carr, Ph.D., Department of Ophthalmology, DMEI #415, The University of Oklahoma Health Sciences Center, 608 Stanton L. Young Blvd., Oklahoma City, OK. 73104, Ph: (405)-271-8784, dan-carr@ouhsc.edu.

lobe hemorrhaging and cingulate gyrus involvement implicating the lateral ventricles as a critical site in the pathogenic process (2, 3). Moreover, enlargement of the lateral ventricles leading to compression of cortical tissue has been shown to correlate with decreased cognitive function suggesting a possible role in the development of acute neurological dysfunction during HSE (4, 5). However, acute ventricle enlargement has not been reported other than in neonatal HSE cases in which a physical obstruction of drainage or overproduction of cerebrospinal fluid (CSF) results in hydrocephalus (6–8).

In the human patient, cytokines including IL-6 and IFN-γ and additional soluble factors including sFas within the CSF are observed in patients diagnozed with HSE (9, 10). Furthermore, enhanced susceptibility to HSE has been described in pre-adolescent populations with genetic mutations in TLR-3 or TLR-3 signaling (11–13) and in a sub-population of rheumatoid arthritic patients treated with TNF-α inhibitors (14). Such findings have begun to identify pathways and molecules ascribed to susceptibility and neuropathogenesis. However, the fundamental series of events that ultimately lead to neuropathology and morbidity associated with HSE in the human patient remain elusive.

Experimental models of HSE have been established in mice with results that suggest inflammation-induced and direct viral-induced pathways as the cause of encephalitis and death following acute infection. For example, $CD4^+$ and $CD8^+$ T cells including $\gamma\delta^+$ T cells contribute to resistance to HSE in that in their absence, mice succumb to infection with greater frequency (15–17). Cytokines secreted by T cells including TNF-α and IFN-γ are protective and reduce the incidence of encephalitis as reported in mice administered exogenous cytokines or in mice deficient in the respective cytokine or cognate cytokine receptor (18–22). Even though the host innate and adaptive immune responses are critical in viral resistance, a fine balance to limit inflammation, on the one hand, yet suppress virus replication and cell death on the other is absolutely necessary in sensitive tissue such as the brain (23, 24). To further explore the relationship between viral insult, predicted anatomical changes within the CNS, and the inflammatory immune response with the development of encephalitis, we chose to incorporate a mouse model of HSE using wild type, type I IFN receptor α chain deficient ($CD118^{-/-}$), and $CD118^{-/-}$ mouse chimeras infected with a highly virulent, neurotropic strain of HSV-1, strain McKrae.

In the current study, we find a pathologic enlargement of the lateral ventricles in mice associated with ependymal cell susceptibility to HSV-1 infection. $CD118^{-/-}$ mouse chimeras demonstrated greater susceptibility to HSV-1. The increased susceptibility correlates with lateral ventricle enlargement which occurs in the host exclusively when the majority of the microglial cell population does not possess a functional type I IFN pathway. Such results indicate a functional type I IFN pathway by resident cells is required to maintain resistance to HSV-1 replication and lateral ventricle pathology during acute infection. Finally, the therapeutic application of a peptide previously reported to alleviate intracranial pressure due to HSV-1 infection (25) suppressed viral-induced lateral ventricle dilation and improved survival of mice. The efficacy was not reflected in changes in viral titer or local CNS inflammation in terms of leukocyte infiltration or cytokine expression. Collectively, we interpret the findings to suggest HSE-induced mortality is the direct result of lateral ventricle enlargement. As such, the treatment of HSE patients with acyclovir along with compounds that lessen ventricular dilation may improve the long-term outlook and diminish the incidence of protracted neurological deficits.

[3]Abbreviations used in this paper: HSE, herpes simplex encephalitis; CSF, cerebral spinal fluid; $CD118^{-/-}$, type I IFN receptor α chain deficient; WT, wild type; PFU, plaque forming units; pi, post infection; BS, brain stem; MRI, magnetic resonance imaging; TK, thymidine kinase; AF-16, anti-secretory factor peptide 16; MMP, matrix metalloproteinase; $TRIF^{-/-}$, TRIF deficient; $MyD88^{-/-}$, MyD88 deficient.

Materials and Methods

Human subject data collection

The study was approved by the Institutional Review Board at the University of Oklahoma Health Sciences Center (Protocol #15984). All data analyzed were anonymized. Patients were identified by retrospective screening of the hospital database for confirmed cases of herpetic encephalitis by ICD9 code (054.3). To identify age and sex matched controls, a query of the picture archiving and communication system (PACS) was performed to identify subjects with reports containing the phrases “normal ventricular size,” “normal ventricles,” and/or “no ventricular enlargement” to be used as “healthy controls.” Controls include both inpatient and outpatient exams. Once records were retrieved, a neuroradiologist examined the MRIs in a masked fashion on two separate occasions to evaluate neuroinflammation proximal to the lateral ventricles and ventricular enlargement. Values were then calculated to obtain a CT Evan’s Index and those above a value of 0.30 were considered pathologic as previously described (26, 27).

$$\text{CT Evan's Index} = \frac{a}{b} = \frac{\text{Maximum axial width of anterior horns of lateral ventricle}}{\text{Maximum intracranial (inner table to inner table)}}$$

Mice and virus

C57BL/6J wild type (WT) [CD45.1 and CD45.2] mice were purchased from Jackson Laboratory and Charles River and housed alongside $CD118^{-/-}$ and $MyD88^{-/-}$ mice (28, 29) in Dean A. McGee Eye Institute’s animal facility. All mice were age- and sex-matched. Animal treatment was consistent with the National Institutes of Health Guidelines on the Care and Use of Laboratory Animals. All experimental procedures were approved by the University of Oklahoma Health Sciences Center and Dean A. McGee Eye Institutes’ Institutional Animal and Care Use Committees. HSV-1 McKrae, HSV-1 GFP (McKrae background), and HSV-1 Tomato Red (KOS background) were propagated Vero cells and maintained at a stock concentration of 10^8 plaque forming unit (PFU)/ml. Anesthetized mice were infected with HSV-1 by applying 3 μl of PBS containing 1,000 to 10,000 PFU of virus as indicated onto the scarified mouse cornea. For plaque assays, at the indicated time pi, tissue and cells were isolated, suspended in 500 μL of RPMI media, and homogenized with a tissue miser for approximately 20–30 seconds. Media was clarified of cellular debris by centrifugation for 60 sec at 10,000 × g. Infectious content within the clarified supernatant was then evaluated as previously described (30).

Magnetic resonance imaging

WT, $CD118^{-/-}$ and mouse chimeras were subjected to gas anesthesia (1.5–2.5% isoflurane, 0.8 L/min O_2). At the indicated time prior to or pi, mice were imaged using a Bruker Biospec 5.0 imaging system to capture T2-weighted images. Volumes of tissue were calculated by drawing regions of interest around consecutive 1 mm slices of T2-weighted images that was then added together for total volume using Paravision software. Four to six mice were analyzed per group.

Cell Culture

A human ependymoma cell line, BXD-1425EPN (31) was maintained in DMEM supplemented with 10% FBS. Once confluency had been reached in tissue culture wells, cells were infected with a multiplicity of infection (MOI) of 0.1 or 0.01. HSV-1 was allowed to adhere for 1 hour at 37°C. After 1 hour, media was changed and 24 hours pi, the medium

was evaluated for infectious content by plaque assay or stained for HSV-1 antigen expression.

Immunohistochemical staining and confocal imaging

WT and CD118$^{-/-}$ mice were anesthetized with ketamine and xylazine and transcardially perfused with 10 mL of cold 4% paraformaldehyde. Brains and livers were removed and fixed for another 48 hrs at room temperature. Samples were then embedded in paraffin blocks and 10 μm sections were cut and mounted on slides. Sections were then subjected to H&E staining or de-paraffinized and blocked overnight at 4°C with donkey serum. Samples to be viewed by confocal microscopy were then subjected to anti-HSV-1 antibody (Dakocytomation) overnight at 4°C. Following 3 washes, secondary antibody (Jackson ImmunoResearch Laboratories) was added overnight at 4°C. Slides were then washed 3 more times and incubated with DAPI overnight. The sections were then imaged with an Olympus IX81-FV500 epiflourescent/confocal laser-scanning microscope as previously described (30).

RT-PCR

At the indicated time pi, the indicated tissues were harvested and resuspended in 500 μL to 1.0 mL of Trizol. Total RNA was then isolated per manufacturer's guidelines (Invitrogen) and semi-quantitative real-time PCR was performed with an iCycler (Bio-Rad) as previously described (32). Primer sequences were as follows:

PRIMER	SEQUENCE
β-actin Forward	5'-CTTCTACAATGAGCTGCGTGTG-3'
β-actin Reverse	5'-TTGAAGGTCTCAAACATGATCTGG-3
IFN-α Foward	5'-CTCATTCTGCAATGACCTCCA-3'
IFN-α Reverse	5'-CCTGATGGTCTTGGTGGTG-3'
IFN-β Forward	5'-CAAGAGGAAAGATTGACGTGG-3'
IFN-β Reverse	5'-TAAGGTACCTTTGCACCCTCC-3'
Oas1a Forward	5'-CTTTGATGTCCTGGGTCATGT-3'
Oas1a Reverse	5'-GCTCCGTGAAGCAGGTAGAG-3'
TK Forward	5'-ATACCGACGATCTGCGACCT-3'
TK Reverse	5'-TTATTGCCGTCATAGCGCGG-3'
TNF-α Forward	5'-CATCTTCTCAAAATTCGAGTGACAA-3'
TNF-α Reverse	5'-TGGGAGTAGACAAGGTACAACCC-3'

Bioplex and ELISA Assays

CSF was accessed through the cisterna magna and collected from uninfected and infected WT and CD118$^{-/-}$ mice at the indicated time pi. Samples were then analyzed by suspension array (Millipore) per manufacturer's protocol for CXCL1, CCL2, CXCL9, CXCL10, IL-1α, and IL-1β. Matrix metalloproteinase 9 levels in the CNS were determined by ELISA (R&D Systems).

Flow Cytometry

At the indicated time pi, brain stem (BS), brain cortex, and ependymal tissue were surgically removed and single cell suspensions were generated using a Wheatley Dounce homogenizer (Fisher Scientific) followed by filtration through a sterile 70 μm cell strainer (BD

Biosciences). Cells were phenotypically characterized following pre-incubation with Fc Block anti-mouse CD16/32 (BD Biosciences) using combinations of fluorochrome-conjugated antibodies to CD3, CD4, CD8, CD11b, CD11c, pan-leukocyte CD45, CD45.1, CD45.2, NK1.1, Gr-1 from BD Biosciences or F4/80 obtained from Serotec using a Coulter Epics XL flow cytometer as previously described (32). In the case of microglia, cells were gated on $CD45^{medium}$ and stained with CD11b. The contribution of resident versus hematopoietic cells in the microglia population in the mouse chimeras was further delineated using anti-CD45.1 or anti-CD45.2 antibody. The percentage of the total microglia population for resident and donor sources is reported.

Brain Slice Culture

WT and $CD118^{-/-}$ mice were transcardially perfused with 10 mls of 1X PBS. Whole brains were then removed, placed in slice media (DMEM, 5% FBS) and sliced into 400 μm transverse sections on a Leica vibratome. Two to three slices were then moved to Millipore organotypic membranes and supplied with 1.2 mls of neural basal media supplemented with B-27, 10% FBS, Hepes, N2, glutamine and glutamax as described (33). Tissue was then inoculated with 1,000–10,000 PFU / slice HSV-1 in 3 μl of neural basal media. After 24 hours, the media was replaced with 1.2 mls of fresh neural basal media without FBS and changed every other day thereafter as described (33). In the indicated experiments, clodronate liposomes or PBS liposome controls were suspended in media at a concentration of 1000 μM and changed every other day with neural basal media. For clodronate experiments, on the second day slices were infected with 10,000 PFU / slice diluted in 3 μL of neural basal media. To confirm slices were viable over the time of experimental manipulation, Presto Blue™ (Invitrogen) was topically applied to slices and incubated for 30 minutes. The slices were then imaged for a color change from blue to red, which indicates tissue viability.

Stereotaxic Inoculation of reporter virus or Evan's blue dye in mice

To directly inoculate HSV-1 expressing tomato red or Evan's blue dye into the lateral ventricles, mice were anesthetized using ketamine and xylazine as previously described. Hair and skin overlaying the skullcap were resected and a pen size hole drilled 0.2 mm caudal and 1.2 mm lateral of the bregma. One thousand PFU of virus or 5 μl of 1% Evan's blue dye was then injected into the lateral ventricles of WT or $CD118^{-/-}$ mice at a depth of 1.0 mm. Uninfected mice served as controls. For HSV infection, skin was then sutured closed and mice were treated with antibiotic-supplemented (trimethoprim and sulfamethazole) water. Seventy-two hours later, mice were sacrificed and brains cut on the vibratome as previously described. For Evan's blue dye experiments, dye was injected into the lateral ventricle and the clearance of the dye (time to the 4^{th} ventricle) was recorded by direct visualization of the dye draining into the cisterna magna with the aide of a dissecting microscope. Mice were then perfused and tissue was then fixed in 4% paraformaldehyde, cut at a thickness of 600 μm, and imaged.

Western Blots

WT organotypic brain slices were cut as previously described at 400μm. The slices were then subjected to clodronate or PBS liposomes as previously described. Twenty-four hrs pi, media and liposomes were changed. Two days later tissue and isolated cells were suspended in Radio-Immunoprecipitation buffer containing protease inhibitors (Santa Cruz) and briefly homogenized with a tissue miser. Protein and nuclear extracts were then isolated, electrophoresed, and transferred onto polyvinylidene fluoride membranes as previously described (30). The membranes were then washed and subjected to primary antibody (GFAP, Invitrogen; NeuroD, Abcam) overnight at 4°C. Following 3 additional washes, samples were incubated with secondary anti-rabbit antibody (Abcam, 1:5000 dilution) for 1

hr at room temparature. The membranes were then washed and signal intensity was evaluated (Pierce) using a Kodak imager. Relative protein expression was then calculated using β-actin or TATA-binding protein as the housekeeping control.

AF-16 Treatment

Anti-secretory factor (AF)-16 peptide (25) with the sequence VCHSKTRSNPENNVGL was synthesized by EZBiolab. Immediately prior to use, the peptide was dissolved in PBS at a concentration of 1.0 mg/ml. CD118$^{-/-}$ and WT mice were infected with either 1,000 or 10,000 PFU / eye HSV-1 respectively. Starting on day 3, mice were anesthetized and treated twice a day with an intranasal injection of 20 μl of AF-16 peptide (1 μg/μl) or PBS through the duration of the experiment up to day 12 pi for WT mice.

Statistical Analysis

Statistical analysis was performed using the GBSTAT one-way analysis of variance followed by an ad hoc Tukey's *t* test in experiments comparing more than two groups, while a Student's *t* test was used to compare two variables. Significance was defined as a p value less than 0.05 throughout the paper.

Results

Magnetic resonance imaging of the brain reveals lateral ventricle involvement in mice and man

We have previously observed CD118$^{-/-}$ mice are highly susceptible to ocular HSV-1 infection with signs consistent with HSE including the absence of grooming, food intake, and neurologic signs (motor dysfunction, including gait, posture, and spontaneous movement) (34, unpublished). Consistent with the appearance of HSE, the viral burden in the cerebral cortex of CD118$^{-/-}$ mice was significantly greater than in WT animals 4 days pi (Fig. 1A) with observable features of encephalitis (35)(Fig. 1B). This trend continued to day 5 pi (Fig. 1A) resulting in severely swollen heads and death of nearly 100% of CD118$^{-/-}$ mice (Fig. 1B). WT mice were not refractory to disease and exhibited similar symptoms as early as 7 days pi but with only an approximate 20% mortality rate (Fig. 1B). As a means to further evaluate global pathology within the CNS, mice were imaged using magnetic resonance imaging (MRI), a useful and non-invasive modality to monitor HSE (36). CD118$^{-/-}$ but not WT mice displayed ventricular enlargement by 5 days pi, which mirrored that of human disease (Fig. 1C, D). This finding was restricted to the lateral ventricles as no overt pathology or enlargement was identified in the third ventricle (Fig. 1C).

Diagnosis of HSE patients typically present with uni- or bilateral cerebro-cortical lesions in the temporal lobe may also include parietal or frontal lobe involvement (37, 38). Since acute ventricle enlargement has previously been reported in neonatal cases of HSE (6–8) and was observed in susceptible CD118$^{-/-}$ mice, we hypothesized this phenomena may occur in a sub-population of HSE adults. In fact, MRI scans of 19 patients with HSE analyzed proximal to tissue within mm of the boundary of the Foramen of Monroe revealed a gross dilatation of the lateral ventricles in 7 patients compared to 0/19 in controls (Fig. 2A, B). While these results were not found to be significant (Fig. 2C), they do suggest that lateral ventricle enlargement may be a feature found in a subpopulation of HSE patients certainly worth further investigation.

HSV-1 targets ependymal cells

Resident cells of the CNS and regions adjacent to lateral ventricles can be infected by HSV-1 *in vitro* and *ex vivo* (39–42). In our *in vivo* encephalitic model, HSV-1 antigen expression was limited to the ependymal cells within the CNS of CD118$^{-/-}$ mice shortly

before or during encephalitis following ocular infection (Fig. 1E). Along with viral tropism to the ependymal region, a loss of ciliated ependymal cells and detection of erythrocytes within the ventricle were also routinely observed in encephalitic CD118$^{-/-}$ mice (Fig. 1E). In a similar fashion, the human ependymoma cell line BXD-1425EPN (31) was found to be highly susceptible to HSV-1 evident by expression of HSV-1 antigen (Fig. 2D) and recovery of progeny virus following infection (Fig. 2E). These results are consistent with the epithelial origin of ependymal cells (43) and high susceptibility of epithelial cells including ependymal cells (44) to HSV-1 infection.

HSV-1 tropism for the ependyma was further substantiated in mice both after direct viral inoculation into the lateral ventricles *in vivo* and *ex vivo* infection of brain slices at sites proximal to the ventricles (Fig. 3). Specifically, stereotaxic placement of tomato red-expressing HSV-1 into the ventricle of WT mice localized selectively to the ependymal region detected within 72 hr post administration (Fig. 3A). In organotypic brain slice cultures, inoculation of ventricle (red asterisk) but not cerebral cortex (blue asterisk) led to the detection of green fluorescent protein expressing reporter virus that localized to the ependymal region (Fig. 3B–D). To identify the selective mode of transit of HSV-1 into the CNS of WT and CD118$^{-/-}$ mice, two routes of entry were considered. HSV may undergo viremia as seen with human immunodeficiency virus (45) and West Nile virus (46) and/or follow neuronal retrograde axonal transport from the periphery such as rabies and West Nile viruses (47, 48). Systemic HSV dissemination has been reported in adults and children (49, 50) and was a plausible route of CNS entry modeled by the rapid spread of virus in CD118$^{-/-}$ mice (34). To test this idea, highly sensitive real time RT-PCR of viral thymidine kinase (TK) was performed on sections of the CNS including the ependyma, cortex, and BS (Fig. 4A) as well as blood samples. TK mRNA expression was detected as early as 3 days pi in the BS and ependymal-rich tissue sections of highly susceptible CD118$^{-/-}$ mice, but was not detected in blood samples until 5 days pi (Fig. 4B, C). In addition, TK expression was detected earlier (day 3 pi) in the ependyma compared to the cortex (day 4 pi) of the CD118$^{-/-}$ mice (Fig. 4B). We interpret the results to suggest HSV-1 enters the CNS through a neural route and rapidly but selectively progresses from the BS to the ependymal cells and then into the cortex.

By comparison, WT mice exhibiting severe symptoms of encephalitis (HSE) were compared to those mice with no overt signs (gait, posture, and spontaneous movement) which routinely occurred at day 8 pi. Viral replication was more pronounced in the ependymal-rich areas of the brain of HSE WT mice for which there was nearly 60-fold more TK transcript relative expression compared to the surrounding cortex (Fig. 4D). Furthermore, there was no difference in the expression of TK in the brain cortex of HSE and non-HSE WT mice at day 8 pi whereas there was approximately 600-fold more TK transcript expressed in the ependymal region of HSE versus non-HSE WT mice (Fig. 4D). Taken together, the results suggest viral levels as measured by TK expression within the ependyma but not cortex of the brain are clearly aligned with encephalitis. This notion is further supported by the expression of TNF-α which was significantly elevated in the ependymal region but not cortex of the brain of HSE but not non-HSE WT mice (Fig. 4D). Ironically, there was no significant difference in the expression of IFN-α or IFN-β in the ependyma or cortex comparing encephalitic to non-encephalitic WT mice (Fig. 4D). Similar to what was found in CD118$^{-/-}$ mice, HSV-1 TK expression was not detected in the blood of WT mice (data not shown) at the time when some WT mice display signs of encephalitis (day 8 pi) suggesting HSV-1 is distributed to the CNS via neuronal routes.

Inflammatory response profile in the CNS of encephalitic CD118$^{-/-}$ and WT mice

Since changes were observed in the expression of the pro-inflammatory cytokine, TNF-α, comparing HSE to non-HSE WT mice, additional experiments were performed to further

identify factors and cell infiltrates associated with HSE. The CSF of HSV-1 infected, HSE CD118$^{-/-}$ mice had detectable levels of IL-1α, CCL2, CXCL1, CXCL9, and CXCL10 compared to uninfected controls at day 5 pi of which CXCL1 and CXCL10 were prominently expressed (Fig. 5A). Likewise, HSE WT mice had detectable levels of IL-1α, CCL2, CXCL1, CXCL9, and CXCL10 with CXCL1 and CXCL10 expression significantly above that recovered in the CSF of non-HSE WT mice day 8 pi (Fig. 5B). Upon analysis of infiltrating cells within the CNS of HSE CD118$^{-/-}$ mice, the ependymal region contained more neutrophils (F4/80^{-}Gr-1^{+}) and total CD45^{hi} leukocytes but not NK cells (NK1.1^{+}CD3^{-}), inflammatory monocytes (F4/80^{+}Gr-1^{+}), or macrophages (F4/80^{+}Gr-1^{-}) compared to brain cortex day 5 pi (Fig. 5C). In comparing HSE to non-HSE WT mice, neutrophils, inflammatory monocytes, macrophages and total leukocyte numbers were all elevated in the HSE WT mice in the brain cortex and ependymal region compared to the non-HSE WT mice (Fig. 5D). Since neutrophils are a highly inflammatory cells and the levels were elevated in the ependymal region of both the HSE CD118$^{-/-}$ and HSE WT mice, we hypothesized neutrophils may be the principal driver of neuropathogenesis and mortality in HSE mice. Therefore, by targeting the neutrophil population, the result may alleviate the host of much of the inflammatory process within the CNS and as a consequence, reduce death. However, anti-Ly6G antibody depletion of neutrophils within the CNS of HSV-1-infected CD118$^{-/-}$ and WT mice did not attenuate the disease course (data not shown) suggesting another pathogenic mechanism.

Lateral ventricle enlargement is detrimental to survival

Increased intracranial pressure is a typical feature of viral encephalitis and has been hypothesized to cause enlargement of the lateral ventricles (51, 52). Thus, we hypothesized that the loss of cilia on ependymal cells of the CD118$^{-/-}$ mice (Fig. 1E) would result in reduced clearance of CSF resulting in the pathogenic expansion of the lateral ventricles seen in both mouse and man that has been previously attributed to parenchymal swelling (51) (Figure 2A). In fact, we found infected CD118$^{-/-}$ mice had a significantly reduced capacity to move dye from the lateral ventricles to the fourth ventricle in comparison to uninfected controls (Fig. 6A, B).

CSF distribution, circulation, and turnover along with intracranial tissue mass influence the intracranial pressure (53). Furthermore, an increase in intracranial pressure can lead to brain herniation and death consistent with outcomes in cases of human HSE (54, 55). To this end, the therapeutic intranasal delivery of a peptide previously reported to reduce intracranial pressure, AF-16 (25), was found to slightly prolong survival of sensitive CD118$^{-/-}$ mice following HSV-1 infection (Fig. 7A, B) but significantly reduce mortality in HSV-1-infected WT mice compared to vehicle-treated controls (Fig. 7C, D). The dramatic improvement in cumulative survival in peptide-treated WT mice correlated with restoration in lateral ventricle volume as indicated in the MRI profile (Fig. 7E, F) and improved neurological signs (data not shown).

AF-16 peptide efficacy does not dampen brain inflammation

As a result of the therapeutic efficacy of the AF-16 peptide applied to HSV-1-infected mice, we next sought to determine the mechanism behind the efficacy. We previously found an elevation in TNF-α, CXCL1, and CXCL10 expressed in the ependyma or CSF as well as an increase in leukocyte infiltrates into the brain of HSE CD118$^{-/-}$ or WT mice compared to non-encephalitic animals (Fig. 4–5). However, analysis of brain cortex and ependyma for cytokine and chemokine (TNF-α and CXCL10) expression by suspension array or leukocyte infiltrate (including neutrophils, macrophages, inflammatory monocytes, and NK cells) by flow cytometry revealed no significant difference in levels or cell numbers comparing peptide- to vehicle-treated mice day 7–8 pi (data not shown). Furthermore, there was no

difference in viral titers recovered from the brain of peptide-treated to vehicle-treated groups day 7–8 pi (data not shown). These results confirm and extend those previously published using an encephalitic rat model (25).

Matrix metalloproteinases (MMP) including MMP-9 but not MMP-2 are associated with an increase in neuropathology during acute HSE (56). Upon comparison of MMP-9 levels in the brain ependyma of peptide- to vehicle-treated, HSV-1 infected mice, we found no difference in total MMP-9 levels which ranged from 50–150 pg/mg tissue. Attempts were made to recover CSF from AF-16 peptide-treated mice to compare levels of inflammatory cytokines. Whereas 3–5 μl of CSF could be recovered in vehicle-treated mice, CSF could not be obtained in peptide-treated mice day 7–8 pi and therefore, no such comparison was possible. As such, the peptide experiment reinforces the detrimental lateral ventricle enlargement as the major pathologic predictor of mouse mortality as evident in the similarities in the inflammatory response and viral loads of AF-16 and PBS-treated groups despite significant differences in survival.

Surveillance of HSV-1 in the brain is due to microglia

Once the virus has infected the tissue lining the lateral ventricles in the CNS, the identification of cells that contribute in resistance against further viral progression remained elusive in WT mice. To first dissect the contribution of resident cells from infiltrating leukocytes, a mouse chimera model was employed. Five days pi, mice with a $CD118^{-/-}$ recipient background regardless of the bone marrow (BM) source had significantly more virus in the CNS, enlarged lateral ventricles, and swollen heads compared to WT mouse recipients of $CD118^{-/-}$ or WT BM (Fig. 8A–D). We interpret these results to suggest a resident cell population such as microglia, astrocytes, and/or neurons afforded protection from HSV-1 infection within the CNS of WT mice.

The microglial cell is thought to be the innate immune cell of the CNS due to its constant surveillance of the tissue (57). In the $CD118^{-/-}$/WT mouse chimera model, a majority of the microglia in the BS and cortex were derived from the original resident population during an uninfected or infected state (Figure 9A–E). Specifically, prior to infection 80–100% of microglia residing in the BS (Fig. 9B) or brain (Fig. 9C) were WT-derived in WT recipients of WT or $CD118^{-/-}$ BM. By comparison, 60–100% of microglia populating the BS or brain of uninfected $CD118^{-/-}$ recipients of WT or $CD118^{-/-}$ BM were $CD118^{-/-}$ derived (Figure 9B, C). Five days following infection, greater than 60% of the microglia in the BS or brain of WT recipients of WT or $CD118^{-/-}$ BM retained the WT phenotype whereas greater than 75% of the microglia in the BS or brain of $CD118^{-/-}$ recipients of WT or $CD118^{-/-}$ BM were of the $CD118^{-/-}$ background (Figure 9D, E). Taken together with the data showing less HSV-1 recovered in the BS or brain of WT recipients of $CD118^{-/-}$ BM in comparison to $CD118^{-/-}$ recipients of WT BM (Fig. 8A), we conclude a resident CNS cell population controls HSV-1 replication within the first 5 days pi.

To exclusively characterize the contribution of resident CNS cells (microglia, astrocytes or neurons) in viral surveillance in a relatively native state in the absence of a leukocyte contribution, an organotypic brain slice culture system was engineered as previously described (33) (Figure 10A). Organotypic brain slice cultures were established from naive WT and $CD118^{-/-}$ mice. Upon infection, the $CD118^{-/-}$ mouse organotypic cultures had significantly more virus than WT cultures confirming a role for IFN-responsive resident cells in the CNS as well as verification that these cultures behaved similar to that seen *in vivo* (Figure 10B). Specific depletion (50% loss) of microglia by clodronate liposomes in WT brain slice cultures (Fig. 10C) resulted in a significant increase in viral titer compared to tissue slices treated with control liposomes (Fig. 10D). Clodronate liposome-mediated depletion of microglia had no apparent effect on astrocytes or neurons as measured by

GFAP or Neuro D expression respectively suggesting microglia were the primary cell population depleted by chlodronate liposome treatment and therefore, responsible for the innate resistance in the brain to HSV-1 infection (Fig. 10E).

Previous reports indicated TLR-3 signaling deficiencies led to an increased susceptibility to HSE in children due to a loss of IFN production (11–13). It has also been reported a loss of this innate sensor renders astrocytes permissive to HSV infection (58). To further investigate this possibility in our model, we evaluated brain slice cultures from TRIF-deficient ($TRIF^{-/-}$), MyD88-deficient ($MyD88^{-/-}$) and WT mice for resistance to primary HSV-1 infection. HSV-1 titers were significantly elevated in the organotypic brain slice cultures from $TRIF^{-/-}$ mice in comparison to the WT and $MyD88^{-/-}$ samples whereas there was no difference comparing WT to $MyD88^{-/-}$ groups (Figure 10F). Furthermore, microglial cell depletion of $TRIF^{-/-}$ mouse brain slice cultures did not enhance susceptibility to HSV infection suggesting the loss of microglia had no further effect on HSV containment in the absence of TRIF (Figure 10G). Thus, TRIF-dependent pathways within microglia were critical to contain HSV-1.

Discussion

In the present article, we found TRIF-activated microglia control viral replication in the CNS of WT mice. In pediatric patients with TLR-3 signaling deficiencies (11–13), the microglial-driven, IFN-β antiviral response is likely compromised and astrocytes are now permissive to viral infection (58). These two findings may explain the susceptibility of these children to recurrent HSV infections of the CNS. In our mouse model of HSE, we found for the first time that a loss of cilia results in a reduced capacity to move CSF through the ventricular network leading to a functional obstruction of fluid movement. This process may be an additional mechanism for acute ventricle enlargement in diseases such as traumatic brain injury and hydrocephalus as the result of previous bacterial meningitis (7, 59). Specifically, reports have shown *Streptococcus pneumoniae*-induced meningitis results in damaged ciliated ependymal cells, reduced cilia cell beat frequency, and is a risk factor for the development of hydrocephalus (60–62). Moreover, traumatic brain injury results in damage to ependymal cells and may result in the development of hydrocephalus (59, 63). The accumulation of CSF and subsequent acute enlargement of the lateral ventricles during HSE has never been reported in adults. We propose such an occurrence may predispose the brain and BS to catastrophic herniation as seen with more typical cases of hydrocephalus (64). Additionally, herniations have been reported during HSE and other viral encephalitises further suggesting viral infections of the CNS increase the probability of brain herniations due to enlargement of the lateral ventricles (65, 66). While CNS herniations of infected mice were not readily appreciable, the rapid decline of $CD118^{-/-}$ mice would suggest this possibility.

Anti-secretory factor, originally described as a protein in the CNS and gut (67) but also found in macrophages (68), was previously found to block cholera toxin-induced intestinal hypersecretion (67). A peptide representing the first 16 amino acids of the anti-secretory factor, AF-16,has previously been reported to enhance HSV-1 infected rat survival which was correlative with a drop in intracranial pressure (25). Therefore, we evaluated the potential use of this peptide in our mouse model of HSE. Consistent with the previous findings, the intranasal application of AF-16 during the acute phase of HSV-1 infection preserved survival and prevented lateral ventricle dilitation. As there is a gross CNS inflammatory response to HSV-1 infection in the brain (69) and soluble factors generated as a result of the infection including MMP-9 and TNF-α are thought to be pathologic (70) or protective (21) respectively to the host, we investigated levels of these and other cytokines as a possible means to further explain the efficacy of the peptide. However, the obvious

possible mediators that might influence the outcome of the infection were unaltered in the peptide-treated mice. Furthermore, we found no change in leukocyte infiltration or in infectious virus content in the brain re-emphasizing the death of the animals was unrelated to viral load or gross inflammation. Rather, it would appear survival is related to maintaining equilibrium between fluid accumulation and clearance evident by lateral ventricle enlargement in this study and intracranial pressure in previously published work (25). The results also emphasize the importance of cilia in bulk flow of CSF (71) and the loss of this fluid movement, we hypothesize, allows localized augmentation in titers of virus to occur. We propose the high viral load is able to overcome the local innate (microglia) immune response allowing HSV access to the surrounding cortex to induce the rapidly progressive disease known as HSE.

Although gross inflammation is not, in and of itself, the driving force behind host survival, we propose CXCL10 as a potential biomarker to delineate magnitude of disease during viral encephalitis. Production of CXCL10 is a well established finding during viral infections of the CNS (72). We found that the amount of CXCL10 detected in the CSF directly correlated with severity of infection in that WT and CD118$^{-/-}$ HSE mouse CSF contained copious amounts of the chemokine. The fact that CSF CXCL10 levels were less in the HSE CD118$^{-/-}$ mice compared to the HSE WT mice may be due to the time in which the samples were obtained (day 8 pi for WT vs day 5 pi for CD118$^{-/-}$ mice) or the relationship between a functional type I IFN pathway and HSV-1-induced CXCL10 (34). We speculate CXCL10 may serve as an easily accessible predictor of inflammation severity in patients with no previous history of neuroinflammatory disease.

In conclusion, we have found in mice deficient in a functional type I IFN pathway, ocular HSV-1 infection results in the rapid spread of the virus to the BS from the cornea. There, the virus traffics to the ependyma, a ciliated, single cell layer lining the lateral ventricles. It is here the virus rapidly replicates destroying the ependymal cells and as a result, increasing fluid accumulation in the lateral ventricles and intracranial pressure that ultimately leads to irreversible brain damage and death of the host. In contrast to CD118$^{-/-}$ mice, WT mice are capable of controlling virus replication and spread to a greater extent although a subpopulation of animals is still prone to develop encephalitis and die. It is clear from the data presented herein viral levels in the ependyma and not the brain cortex correlate with severity of the disease state, and that microglia are the principal resident cell source that is required for viral surveillance in a TRIF-dependent manner. Whereas it is likely TRIF activation is mediated via the TLR3 sensor, we have not formally excluded TLR4 which can also signal through TRIF (73). Likewise, TLR-independent sensors including DNA-dependent activator of interferon regulator factor and IFI16/p204 that respond to HSV-1 may also contribute to viral surveillance in the CNS and specifically, in the ependymal region (30, 74). Ultimately, these pathways converge in the generation of type I IFNs that counter HSV-1 replication and thus, would reduce tissue pathology and preserve the ependymal cell lining of the lateral ventricles. We presume the lack of a difference in type I IFN expression in the ependyma region of encephalitic compared to non-encephalitic WT mice was due to the time analyzed (day 8 pi) due to the clinical presentation of the animal. Earlier time points could not be predicted based on the phenotype of individual WT mice. Future work is required to more fully address this unproven hypothesis and potentially apply such findings to therapy in the human condition.

Acknowledgments

The authors would like to thank Spencer Kwak and Drs. Ana Chucair-Elliott, Sabrina Doblas, Nataliya Smith, and John Ash for technical assistance. We would also like to thank Dr. William P. Halford for fluorescent expressing HSV-1 strains. The authors would also like to thank Drs. Helen Rosenberg and Shizuro Akira for the CD118$^{-/-}$ and MyD88$^{-/-}$ mice respectively. The authors acknowledge Dr. Xiao-Nan Li for the human ependymoma cells.

Finally, the authors acknowledge Drs. Robyn Klein and Jenny LaVail for critical reading and discussion regarding to the findings in the manuscript.

References

1. Conrady CD, Drevets DA, Carr DJJ. Herpes simplex type 1 (HSV-1) infection of the nervous system: is an immune response a good thing? J. Neuroimmunol. 2010; 220:1–9. [PubMed: 19819030]
2. Sellner J, Buonomano R, Nedeltchev K, Findling O, Schroth G, Surbek DV, Leib SL. A case of maternal herpes simplex virus encephalitis during late pregnancy. Nat. Clin. Pract. Neurol. 2009; 5:51–56. [PubMed: 19129790]
3. Kennedy PG, Chaudhuri A. Herpes simplex encephalitis. J. Neurol. Neurosurg. Psychiatry. 2002; 73:237–238. [PubMed: 12185148]
4. Breteler MM, van Amerongen NM, van Swieten JC, Claus JJ, Grobbee DE, van Gijn J, Hofman A, van Harskamp F. Cognitive correlates of ventricular enlargement and cerebral white matter lesions on magnetic resonance imaging. The Rotterdam Study. Stroke. 1994; 25:1109–1115. [PubMed: 8202966]
5. Raschilas F, Wolff M, Delatour F, Chaffaut C, De Broucker T, Chevret S, Lebon P, Canton P, Rozenberg F. Outcome of and prognostic factors for herpes simplex encephalitis in adult patients: results of a multicenter study. Clin. Infect. Dis. 2002; 35:254–260. [PubMed: 12115090]
6. Corey L, Wald A. Maternal and neonatal herpes simplex virus infections. New Engl. J. Med. 2009; 361:1376–1385. [PubMed: 19797284]
7. Tyagi A, Chumas P, Ferrie C. Obstructive hydrocephalus following herpes simplex virus type 1 encephalitis treated by repeated third ventriculostomy. Pediatr. Neurosurg. 2001; 34:244–246. [PubMed: 11423775]
8. Lindeman GJ, Dagnino L, Gaubatz S, Xu Y, Bronson RT, Warren HB, Livingston DM. A specific, nonproliferative role for E2F-5 in choroid plexus function revealed by gene targeting. Genes Dev. 1998; 12:1092–1098. [PubMed: 9553039]
9. Aurelius E, Andersson B, Forsgren M, Skoldenberg B, Strannegard O. Cytokines and other markers of intrathecal immune response in patients with herpes simplex encephalitis. J. Infect. Dis. 1994; 170:678–681. [PubMed: 8077727]
10. Sabri F, Granath F, Hjalmarsson A, Aurelius E, Skoldenberg B. Modulation of sFas indicates apoptosis in human herpes simplex encephalitis. J. Neuroimmunol. 2006; 171:171–176. [PubMed: 16325272]
11. Zhang S-Y, Jouanguy E, Ugolini S, Smahi A, Elain G, Romero P, Segal D, Sancho-Shimizu V, Lorenzo L, Puel A, Picard C, Chapgier A, Plancoulaine S, Titeux M, Cognet C, von Bernuth H, Ku C-L, Casrouge A, Zhang X-X, Barreiro L, Leonard J, Hamilton C, Lebon P, Heron B, Vallee L, Quintana-Murci L, Hovnanian A, Rozenberg F, Vivier E, Geissmann F, Tardieu M, Abel L, Casanova J-L. TLR3 deficiency in patients with herpes simplex encephalitis. Science. 2007; 317:1522–1527. [PubMed: 17872438]
12. Guo Y, Audry M, Ciancanelli M, Alsina L, Azevedo J, Herman M, Anguino E, Sancho-Shimizu V, Lorenzo L, Pauwels E, Philippe PB, Perez de Diego R, Cardon A, Vogt G, Picard C, Andrianirina ZZ, Rozenberg F, Lebon P, Plancoulaine S, Tardieu M, Doireau V, Jouanguy E, Chaussabel D, Geissmann F, Abel L, Casanova J-L, Zhang SY. Herpes simplex virus encephalitis in a patient with complete TLR3 deficiency: TLR3 is otherwise redundant in protective immunity. J. Exp. Med. 2011; 208:2083–2098. [PubMed: 21911422]
13. Sancho-Shimizu, Perez de Diego R, Lorenzo L, Halwani R, Alangari A, Israelsson E, Fabrega S, Cardon A, Maluenda J, Tatemasu M, Mahvelati F, Herman M, Ciancanelli M, Guo Y, Alsum Z, Alkhamis N, Al-Makadma AS, Ghadiri A, Boucherit S, Plancoulaine S, Picard C, Rozenberg F, Tardieu M, Lebon P, Jouanguy E, Rezaei N, Seya T, Matsumoto M, Chaussabel D, Puel A, Zhang SY, Abel L, Al-Muhsen S, Casanova J-L. J. Clin. Invest. 121:4889–4902. [PubMed: 22105173]
14. Bradford RD, Pettit AC, Wright PW, Mulligan MJ, Moreland LW, McLain DA, Gnann JW, Bloch KC. Herpes simplex encephalitis during treatment with tumor necrosis factor-α inhibitors. Clin. Infect. Dis. 2009; 49:924–927. [PubMed: 19681709]

15. Sciammas R, Kodukula P, Tang Q, Hendricks RL, Bluestone JA. T cell receptor-γ/δ cells protect mice from herpes simplex type 1-induced lethal encephalitis. J. Exp. Med. 1997; 185:1969–1975. [PubMed: 9166426]
16. Noisakran S, Carr DJJ. The antiviral efficacy of the murine alpha-1 interferon transgene against ocular herpes simplex virus type 1 requires the presence of CD4(+), alpha/beta T-cell receptor-positive T lymphocytes with the capacity to produce gamma interferon. J. Virol. 2002; 76:9398–9406. [PubMed: 12186922]
17. Anglen CS, Truckenmiller ME, Schell TD, Bonneau RH. The dual role of CD8+ T lymphocytes in the development of stress-induced herpes simplex encephalitis. J. Neuroimmunol. 2002; 140:13–27. [PubMed: 12864968]
18. Rossol-Voth R, Rossol S, Schutt KH, Corridori S, de Cian W, Falke D. *In vivo*protective effect of tumor necrosis factor α against experimental infection with herpes simplex virus type 1. J. Gen. Virol. 1991; 72:143–147. [PubMed: 1703559]
19. Cantin E, Tanamachi B, Openshaw H, Mann J, Clarke K. Gamma interferon (IFN-γ) receptor null-mutant mice are more susceptible to herpes simplex virus type 1 infection than IFN-γ ligand null-mutant mice. J. Virol. 1999; 73:5196–5200. [PubMed: 10233988]
20. Sergerie Y, Rivest S, Boivin G. Tumor necrosis factor-α and interleukin-1β play a critical role in the resistance against lethal herpes simplex virus encephalitis. J. Infect. Dis. 2007; 196:853–860. [PubMed: 17703415]
21. Lundberg P, Welander PV, Edwards CK III, van Rooijen N, Cantin E. Tumor necrosis factor (TNF) protects resistant C57BL/6 mice against herpes simplex virus-induced encephalitis independently of signaling via TNF receptor 1 or 2. J. Virol. 2007; 81:1451–1460. [PubMed: 17108044]
22. Vilela MC, Lima GK, Rodrigues DH, Lacerda-Queiroz N, Mansur DS, de Miranda AS, Rachild MA, Kroon EG, Vieira LQ, Campos MA, Teixeira MM, Teixeira AL. TNFR1 plays a critical role in the conrol of severe HSV-1 encephalitis. Neurosci. Lett. 2010; 479:58–62. [PubMed: 20478363]
23. Kurt-Jones EA, Chan M, Zhou S, Wang J, Reed G, Bronson R, Arnold MM, Knipe DM, Finberg RW. Herpes simplex virus 1 interaction with toll-like receptor 2 contributes to lethal encephalitis. Proc. Natl. Acad. Sci. USA. 2004; 101:1315–1320. [PubMed: 14739339]
24. Lundberg P, Ramakrishna C, Brown J, Tyszka JM, Hamamura M, Hinton DR, Kovats S, Nalcioglu O, Weinberg K, Openshaw H, Cantin EM. The immune response to herpes simplex virus type 1 infection in susceptible mice is a major cause of central nervous system pathology resulting in fatal encephalitis. J. Virol. 2008; 82:7078–7088. [PubMed: 18480436]
25. Jennische E, Bergström T, Johansson M, Nyström K, Tarkowski A, et al. The peptide AF-16 abolishes sickness and death at experimental encephalitis by reducing increase of intracranial pressure. Brain Res. 2008; 1227:189–197. [PubMed: 18586012]
26. Garcia-Valdecasas-Campelo E, González-Reimers E, Santolaria-Fernández F, De La Vega-Prieto MJ, Milena-Abril A, Sánchez-Pérez MJ, Martínez-Riera A, Rodríguez-Rodríguez E. Brain atrophy in alcoholics: relationship with alcohol intake; liver disease; nutritional status, and inflammation. Alcohol Alcohol. 2007; 42:533–538. [PubMed: 17855333]
27. Ambarki K, Israelsson H, Wåhlin A, Birgander R, Eklund A. Brain ventricular size in healthy elderly: comparison between Evans index and volume measurement. Neurosurgery. 2010; 67:94–99. [PubMed: 20559096]
28. Garvey TL, Dyer KD, Ellis JA, Bonville CA, Foster B, Prussin C, Easton AJ, Domachowske JB, Rosenberg HF. Inflammatory responses to pneumovirus infection in IFN-alpha beta R gene-deleted mice. J. Immunol. 2005; 175:4735–4744. [PubMed: 16177121]
29. Adachi O, Kawai T, Takeda K, Matsumoto M, Tsutsui H, Sakagami M, Nakanishi K, Akira S. Targeted disruption of the MyD88 gene results in loss of IL-1- and IL-18-mediated function. Immunity. 1998; 9:143–150. [PubMed: 9697844]
30. Conrady CD, Zheng M, Fitzgerald KA, Liu C, Carr DJJ. Resistance to HSV-1 infection in the epithelium resides with the novel innate sensor, IFI-16. Mucosal Immunol. 2012; 5:173–183. [PubMed: 22236996]
31. Yu L, Baxter PA, Voicu H, Gurusiddappa S, Zhao Y, Adesina A, Man TK, Shu Q, Zhang YJ, Zhao XM, Su JM, Perlaky L, Dauser R, Chintaqumpala M, Lau CC, Blaney SM, Rao PH, Leung HC, Li

XN. A clinically relevant orthotopic xenograft model of ependymoma that maintains the genomic signature of the primary tumor and preserves cancer stem cells in vivo. Neuro. Oncol. 2010; 12:580–594. 2010. [PubMed: 20511191]

32. Wuest TR, Carr DJJ. Dysregulation of CXCR3 signaling due to CXCL10 deficiency impairs the antiviral response to herpes simplex virus 1 infection. J. Immunol. 2008; 181:7985–7993. [PubMed: 19017990]
33. Dionne KR, Leser JS, Lorenzen KA, Beckham JD, Tyler KL. A brain slice culture model of viral encephalitis reveals an innate CNS cytokine response profile and the therapeutic potential of caspase inhibition. Exp. Neurol. 2011; 228:222–231. [PubMed: 21241693]
34. Conrady CD, Thapa M, Wuest T, Carr DJJ. Loss of mandibular lymph node integrity is associated with an increase in sensitivity to HSV-1 infection in CD118-deficient mice. J. Immunol. 2009; 182:3678–3687. [PubMed: 19265146]
35. He Z. Fluorogold induces persistent neurological deficits and circling behavior in mice over-expressing human mutant tau. Curr. Neurovasc. Res. 2009; 6:54–61. [PubMed: 19355926]
36. Meyding-Lamade U, Lamade W, Kehm R, Knopf KW, Hess T, Gosztonyi G, Degen O, Hacke W. Herpes simplex virus encephalitis: cranial magnetic resonance imaging and neuropathology in a mouse model. Neurosci. Lett. 1998; 248:13–16. [PubMed: 9665652]
37. Whitley RJ. Herpes simplex encephalitis: adolescents and adults. Antiviral Res. 2006; 71:141–148. [PubMed: 16675036]
38. Sabah M, Mulcahy J, Zeman A. Herpes simplex encephalitis. B.M.J. 2012; 344:e3166.
39. Aravalli RN, Hu S, Rowen TN, Palmquist JM, Lokensgard JR. Cutting edge: TLR2-mediated proinflammatory cytokine and chemokine production by microglial cells in response to herpes simplex virus. J. Immunol. 2005; 175:4189–4193. [PubMed: 16177057]
40. McCarthy M, Norenberg MD, Norenberg LO, Dix RD. Herpes simplex virus type 1 infection of rat astrocytes in primary culture: effects of dibutyryl cyclic AMP. J. Neuropathol. Exp. Neurol. 1990; 49:3–20. [PubMed: 2153759]
41. Richart SM, Simpson SA, Krummenacher C, Whitbeck JC, Pizer LI, Cohen GH, Eisenberg RJ, Wilcox CL. Entry of herpes simplex virus type 1 into primary sensory neurons in vitro is mediated by Nectin-1/HveC. J Virol. 2003; 77:3307–3311. [PubMed: 12584355]
42. Cohen M, Braun E, Tsalenchuck Y, Panet A, Steiner I. Restrictions that control herpes simplex virus type 1 infection in mouse brain ex vivo. J. Gen. Virol. 2011; 92:2383–2393. [PubMed: 21697348]
43. Doetsch F, Garcia-Verdugo JM, Alvarez Buylla A. Cellular composition and three-dimensional organization of the subventricular germinal zone in the adult mammalian brain. J. Neurosci. 1997; 17:5046–5061. [PubMed: 9185542]
44. Tardieu M, Weiner HL. Viral receptors on isolated murine and human ependymal cells. Science. 1982; 215:419–421 . [PubMed: 6276976]
45. McGavern DB, Kang SS. Illuminating viral infections in the nervous system. Nat. Rev. Immunol. 2011; 11:318–329. [PubMed: 21508982]
46. Wang T, Town T, Alexopoulou L, Anderson JF, Fikrig E, Flavell RA. Toll-like receptor 3 mediates West Nile virus entry into the brain causing lethal encephalitis. Nat. Med. 2004; 10:1366–1373. [PubMed: 15558055]
47. Preuss MA, Faber ML, Tan GS, Bette M, Dietzschold B, Weihe E, Schnell MJ. Intravenous inoculation of a bat-associated rabies virus causes lethal encephalopathy in mice through invasion of the brain via neurosecretory hypothalamic fibers. PLoS Pathog. 2009; 5:e1000485. [PubMed: 19543379]
48. Samuel MA, Wang H, Siddharthan V, Morrey JD, Diamond MS. Axonal transport mediates West Nile virus entry into the central nervous system and induces acute flaccid paralysis. Proc. Natl. Acad. Sci. USA. 2007; 104:17140–17145. [PubMed: 17939996]
49. Harel L, Smetana Z, Prais D, Book M, Alkin M, et al. Presence of viremia in patients with primary herpetic gingivostomatitis. Clin. Infect. Dis. 2004; 39:636–640. [PubMed: 15356775]
50. Young EJ, Killam AP, Greene JF Jr. Disseminated herpesvirus infection. Association with primary genital herpes in pregnancy. JAMA. 1976; 235:2731–2733. [PubMed: 178938]

51. Kumar G, Kalita J, Misra UK. Raised intracranial pressure in acute viral encephalitis. Clin.Neurol. Neurosurg. 2009; 111:399–406. [PubMed: 19372001]
52. Takagi H, Tamaki Y, Morii S, Ohwada T. Rapid enlargement of ventricles within seven hours after head injury. Surg. Neurol. 1981; 16:103–105. [PubMed: 7280980]
53. Brodbelt A, Stoodley M. CSF pathways: a review. Brit. J. Neurosurg. 2007; 21:510–520. [PubMed: 17922324]
54. Tyler KL. Herpes simplex virus infections of the central nervous system: encephalitis and meningitis including Mollaret's. Herpes. 2004; 11:57A–64A.
55. Whitley RJ. Herpes simplex encephalitis: adolescents and adults. Antiviral Res. 2006; 71:141–148. [PubMed: 16675036]
56. Sellner J, Simon F, Meyding-Lamande U, Leib SL. Herpes-simplex viurs encephalitis is characterized by an early MMP-9 increase and collagen type IV degradation. Brain Res. 2006; 1125:155–162. [PubMed: 17109833]
57. Nimmerjahn A, Kirchhoff F, Helmchen F. Resting microglial cells are highly dynamic surveillants of brain parenchyma in vivo. Science. 2005; 308:1314–1318. [PubMed: 15831717]
58. Reinert LS, Harder L, Holm CK, Iversen MB, Horan KA, et al. TLR3 deficiency renders astrocytes permissive to herpes simplex virus infection and facilitates establishment of CNS infection in mice. J. Clin. Invest. 2012; 122:1368–1376. [PubMed: 22426207]
59. Meyers CA, Levin HS, Eisenberg HM, Guinto FC. Early versus late lateral ventricular enlargement following closed head injury. J. Neurol. Neurosurg. Psychiatry. 1983; 46:1092–1097. [PubMed: 6607318]
60. Hirst RA, Sikand KS, Rutman A, Mitchell TJ, Andrew PW, et al. Relative roles of pneumolysin and hydrogen peroxide from Streptococcus pneumoniae in inhibition of ependymal ciliary beat frequency. Infect. Immun. 2000; 68:1557–1562. [PubMed: 10678974]
61. Hirst RA, Mohammed BJ, Mitchell TJ, Andrew PW, O'Callaghan C. Streptococcus pneumoniae-induced inhibition of rat ependymal cilia is attenuated by antipneumolysin antibody. Infect. Immun. 2004; 72:6694–6698. [PubMed: 15501805]
62. Kastenbauer S, Pfister HW. Pneumococcal meningitis in adults: spectrum of complications and prognostic factors in a series of 87 cases. Brain. 2003; 126:1015–1025. [PubMed: 12690042]
63. Johanson C, Stopa E, Baird A, Sharma H. Traumatic brain injury and recovery mechanisms: peptide modulation of periventricular neurogenic regions by the choroid plexus-CSF nexus. J. Neural Transm. 2011; 118:115–133. [PubMed: 20936524]
64. Fleck SK, Baldauf J, Langner S, Rosenstengel C, Siegfried Schroeder HW. Tonsillar herniation and syringomyelia caused by long-standing occlusive hydrocephalus due to aqueductal stenosis: rapid resolution after endoscopic third ventriculostomy--a case report. J. Neurol. Neurosurg. Psychiatry. 2012; 83:343–344. [PubMed: 21317417]
65. Solomon T, Dung NM, Kneen R, Thao le TT, Gainsborough M, et al. Seizures and raised intracranial pressure in Vietnamese patients with Japanese encephalitis. Brain. 2002; 125:1084–1093. [PubMed: 11960897]
66. Ebel H, Kuchta J, Balogh A, Klug N. Operative treatment of tentorial herniation in herpes encephalitis. Childs Nerv. Syst. 1999; 15:84–86. [PubMed: 10230661]
67. Lonnroth I, Lange S. Purification and characterization of the antisecretory factor: a protein in the central nervous system and in the gut which inhibits intestinal hypersecretion induced by cholera toxin. Biochim. Biophys. Acta. 1986; 883:138–144. [PubMed: 3524692]
68. Davidson TS, Hickey WF. Distribution and immunoregulatory properties of antisecretory factor. Lab. Invest. 2004; 84:307–319. [PubMed: 14767482]
69. Marques CP, Cheeran MC, Palmquist JM, Hu S, Urban SL, Logensgard JR. Prolonged microglial cell activation and lymphocyte infiltration following experimental herpes encephalitis. J. Immunol. 2008:6417–6426. [PubMed: 18941232]
70. Zhou, Lu YZN, Guo YJ, Mei YW. Favorable effects of MMP-9 knockdown in murine herpes simplex virus encephalitis using small interfering RNA. Neural Res. 2010; 32:801–809.
71. Del Bigio MR. The ependyma: a protective barrier between brain and cerebrospinal fluid. Glia. 1995; 14:1–13. [PubMed: 7615341]

72. Klein RS, Lin E, Zhang B, Luster AD, Tollett J, et al. Neuronal CXCL10 directs CD8+ T-cell recruitment and control of West Nile virus encephalitis. J. Virol. 2005; 79:11457–11466. [PubMed: 16103196]

73. Yamamoto M, Sato S, Mori K, Hoshino K, Takeuchi O, Takeda K, Akira S. Cutting Edge: a novel Toll/IL-1 receptor domain-containing adapter that preferentially activates the IFN-beta promoter in the Toll-like recepptor signaling. J. Immunol. 2002; 169:6668–6672. [PubMed: 12471095]

74. Furr SR, Chauhan VS, Moerdyk-Schauwecker MJ, Marriott I. A role for DNA-dependent activator of interferon regulatory factor in the recognition of herpes simplex virus type 1 by glial cells. J. Neuroinflammation. 2011

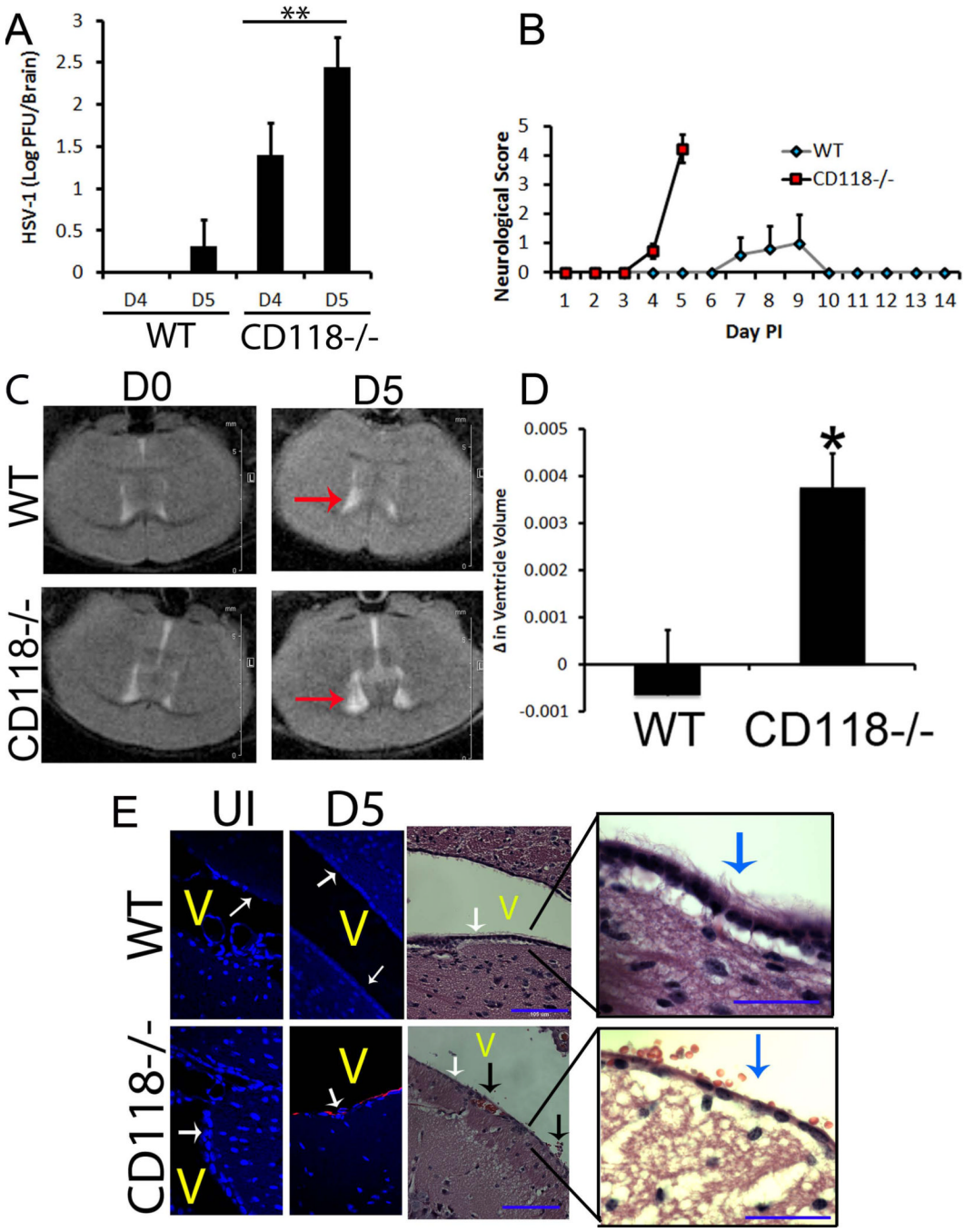

Figure 1.

CD118$^{-/-}$ mice suffer from lateral ventricle involvement. (**A–D**) WT and CD118$^{-/-}$ mice were evaluated for viral content (**A**), overt encephalitic symptoms (**B**), and *in vivo* pathology (**C, D**) following ocular HSV-1 infection (1,000 pfu/eye). Values are the mean ± SEM. n = 4–5 mice per group; red arrows, lateral ventricles; *p < 0.05; **p<.01. (**E**) To identify the precise location of HSV antigen (red) and surrounding pathology, immunostaining and H & E images were captured. White arrows in fluorescent images, ependymal layer; white/blue arrows in H & E, cilia; black arrows, subependymal hemorrhaging (RBCs in CSF fluid); V, ventricle. n = 4–5 mice / group. Blue bar, 105 μm.

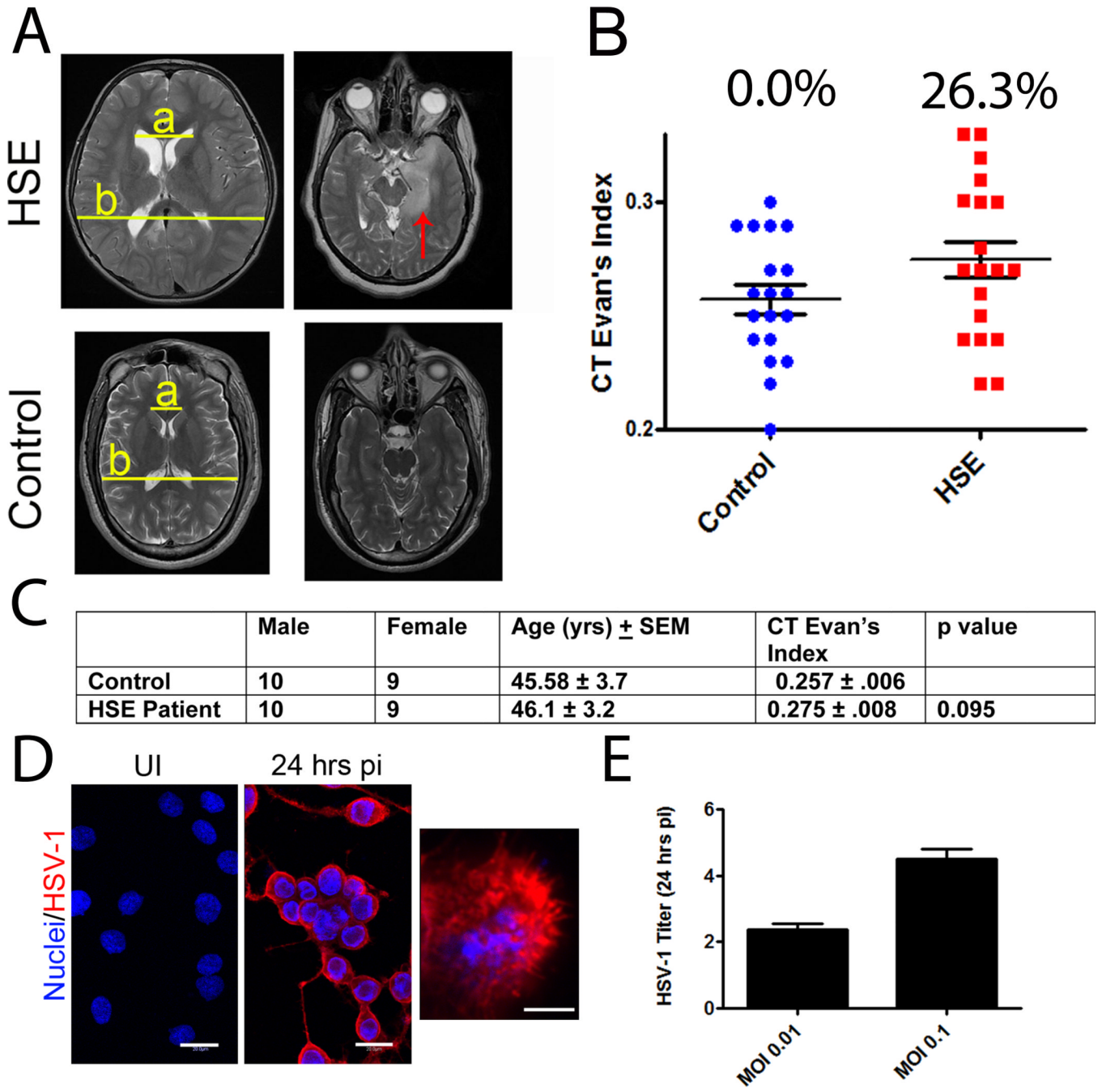

	Male	Female	Age (yrs) ± SEM	CT Evan's Index	p value
Control	10	9	45.58 ± 3.7	0.257 ± .006	
HSE Patient	10	9	46.1 ± 3.2	0.275 ± .008	0.095

Figure 2.

Lateral ventricle enlargement in human HSE. (**A–B**) Left images: Ventricle size was compared between HSE patients and controls at the Foramen of Monroe and is presented as the mean CT Evan's Index ± SEM. CT Evan's index was calculated as the ratio of a/b. Pathologic ventricle enlargement was defined as an index greater than 0.30. "a", maximum width of the lateral ventricles; "b", maximal intracranial width same image. Right images: Axial images of the temporal lobe demonstrate mesial temporal lobe edema (red arrow) characteristic of HSE. (**C**) Patient demographics. (**D–E**) Human ependymoma cells were infected with HSV-1 at an MOI of either 0.1 or 0.01 and expressed antigen (in red) (**D**) and reproduced infectious virus 24 hrs pi (**E**). Images are representative of 2 independent

experiments. Results are presented as the mean log PFU ± SEM. White bars, 20 μm; UI, uninfected.

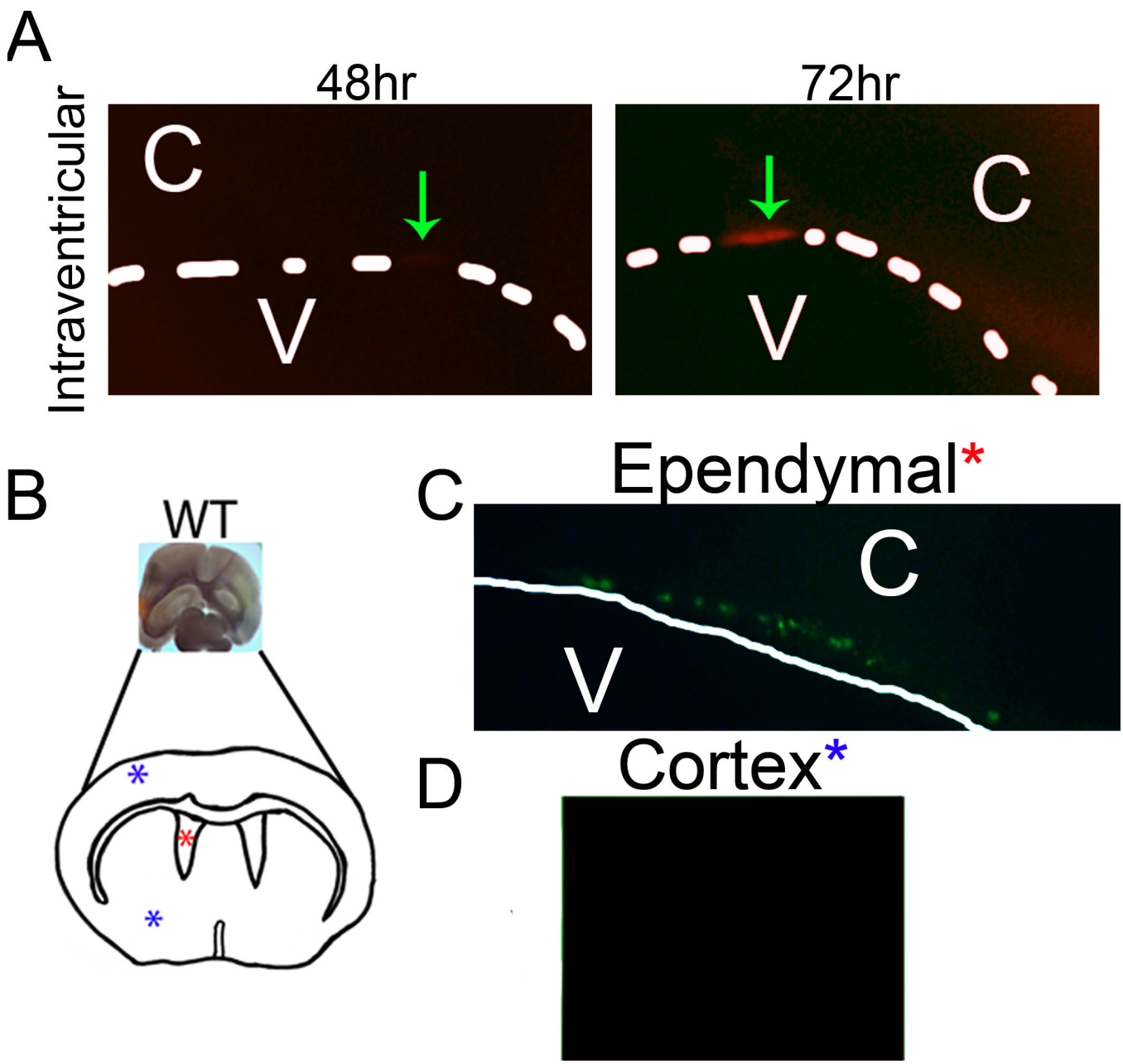

Figure 3.

HSV infection results in ependymal inoculation. (**A**) To confirm infection of ependymal cells, tomato red expressing HSV-1 was directly inoculated into the lateral ventricles. Two days pi WT brains were isolated, sectioned on a vibratome, and imaged for consecutive days for tomato red expression. Green arrows, area of tomato red expression. (**B–D**) To substantiate infection of ependymal cells, WT brain slices were infected with GFP-expressing HSV in either the cortex (**D**) or ependymal area (**C**). Slices were then imaged 2 days pi for GFP expression. C, cortex; V, ventricle; dotted white line, ependymal cell layer; white arrow, infected ependymal cells. Images are representative of 2–3 independent experiments.

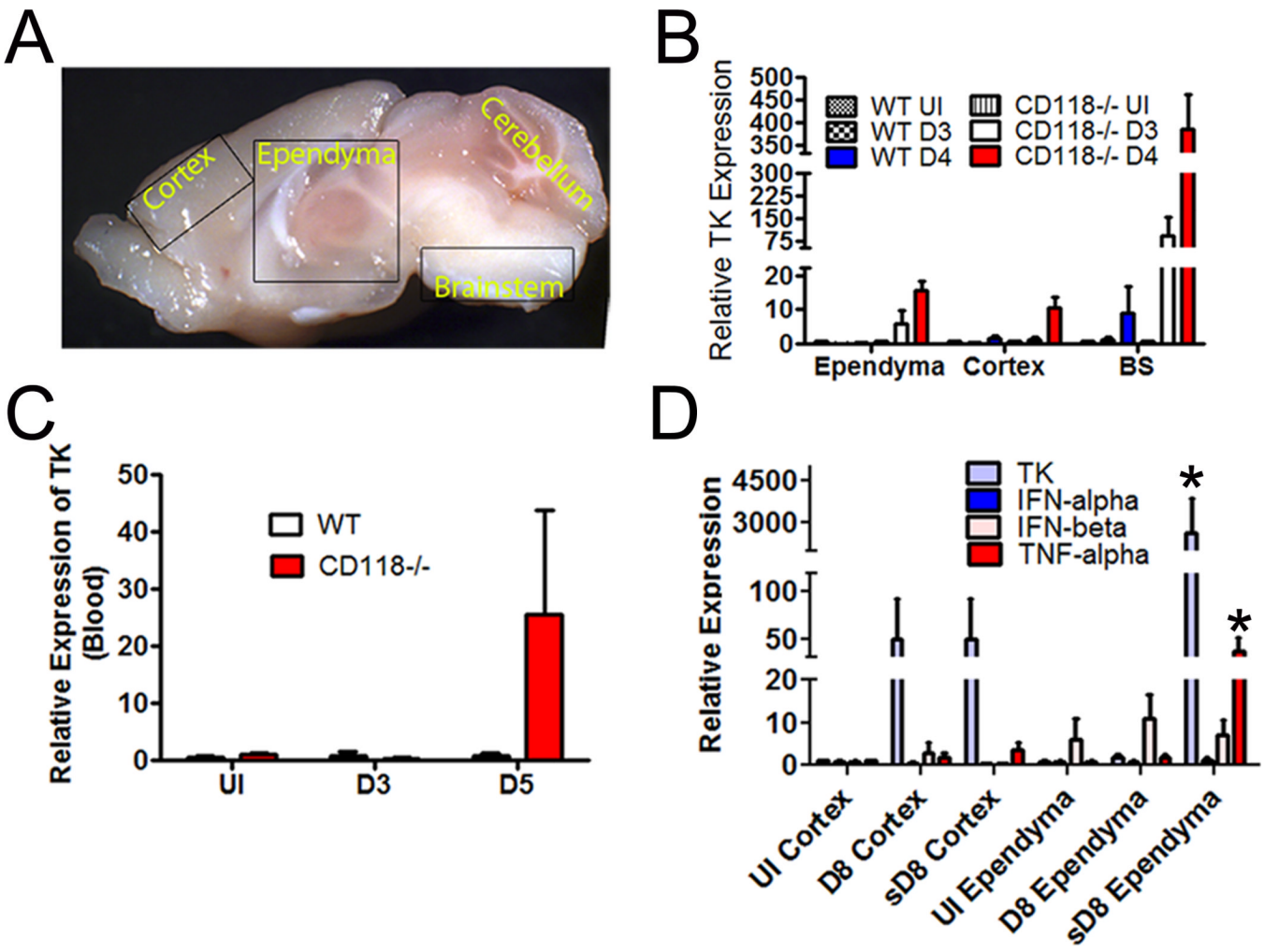

Figure 4.

HSV-1 targets the ependyma via neural projections rather than by a hematogenous route. (**A**) Anatomical location of the ependyma relative to cortex, cerebellum, and brain stem of mouse. (**B**) Viral TK mRNA expression detected in the ependyma, cortex, and BS of WT and CD118$^{-/-}$ mice comparing uninfected (UI) mice to mice infected with 1,000 PFU/cornea and assessed at day 3 (D3) or day 4 (D4) pi. Values are the mean ± SEM. n = 4–6 mice/group. (**C**) Viral TK mRNA expression detected in the blood of HSV-1-infected mice at the indicated time pi. Values are the mean ± SEM. n = 4–6 mice/group. (**D**) WT mice were infected with 1,000 PFU/cornea HSV-1. Eight days pi, relative expression of TK, IFN-α, IFN-β, and TNF-α in the cortex or ependymal region of extremely sick (encephalitic) mice (“s”) and those not exhibiting signs of encephalitis were evaluated and normalized to the housekeeping gene β-actin. Uninfected (UI) mice served as controls. The results are expressed as the mean ± SEM of 3 independent experiments of 1–4 mice/group/experiment. *p<.05 comparing sD8 ependyma group to UI and D8 ependyma groups.

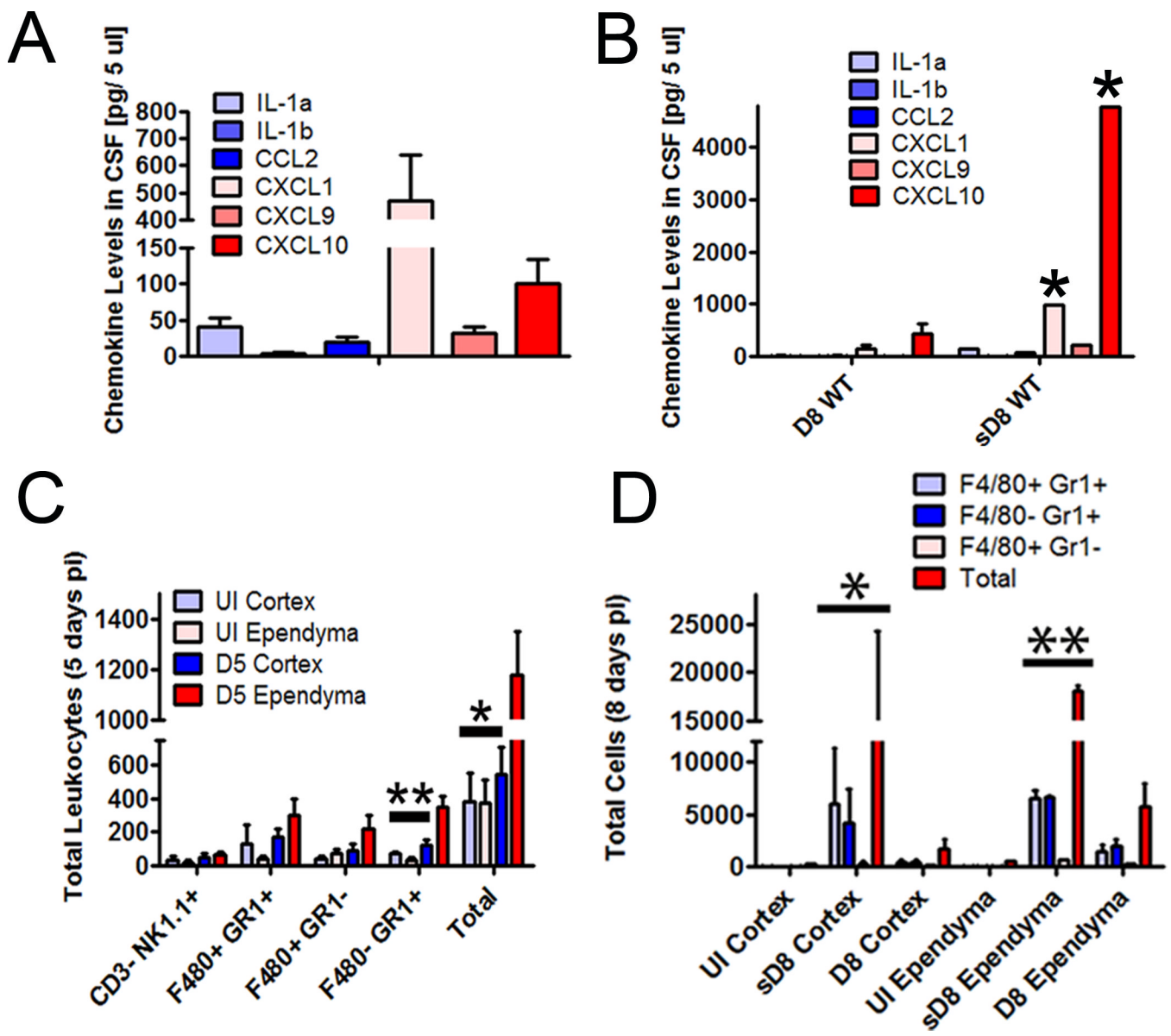

Figure 5.

Inflammatory profile in the CNS of HSE CD118$^{-/-}$ and WT mice to non-HSE WT mice. In all cases, mice were infected with 1,000 PFU/cornea HSV-1. (**A**) Uninfected and infected CD118$^{-/-}$ mice CSF (n=5/group) was isolated and evaluated for select pro-inflammatory cytokines and chemokines by suspension array. Uninfected CSF levels for each analyte measured were as follows (expressed as the mean in pg/5 μl CSF): IL-1α, 19.4; IL-1β, 0.0; CCL2, 12.1; CXCL1, 169; CXCL9, 4.0; and CXCL10, 38. Uninfected levels served as background levels and were subtracted from the levels detected in the infected CD118$^{-/-}$ mice. Levels are expressed as mean ± SEM. With the exception of IL-1β, all analyte levels in the infected CD118$^{-/-}$ were significantly above those found in uninfected CD118$^{-/-}$ mice. (**B**) Same as A except comparing HSE (s) to non-HSE WT mice in which CSF was extracted from the mice day 8 (D8) pi. Levels are expressed as mean ± SEM. *p<0.05 comparing HSE to non-HSE CSF samples for CXCL1 and CXCL10. (**C**) Leukocyte infiltration was evaluated in serial dissections of ependymal-enriched regions and cortex of uninfected (UI) and infected CD118$^{-/-}$ mice euthanized at day 5 pi (D5) by flow cytometry.

The data is expressed as mean ± SEM. **p<.01, *p<.05 comparing the day 5 pi ependymal-enriched group to the day 5 pi cortex and UI ependymal-enriched and cortex groups. (**D**) Leukocyte infiltration was evaluated as in C in WT mice (n=4–12/group summarized from three experiments) with overt symptoms of HSE (abbreviated “s”) compared to those with no HSE clinical presentation within the cortex and ependymal-enriched region by flow cytometry day 8 (D8) pi. The data is expressed as mean ± SEM. **p<.01, *p<.05 comparing the HSE ependymal-enriched and cortex groups to the non-HSE and UI ependymal-enriched and cortex groups.

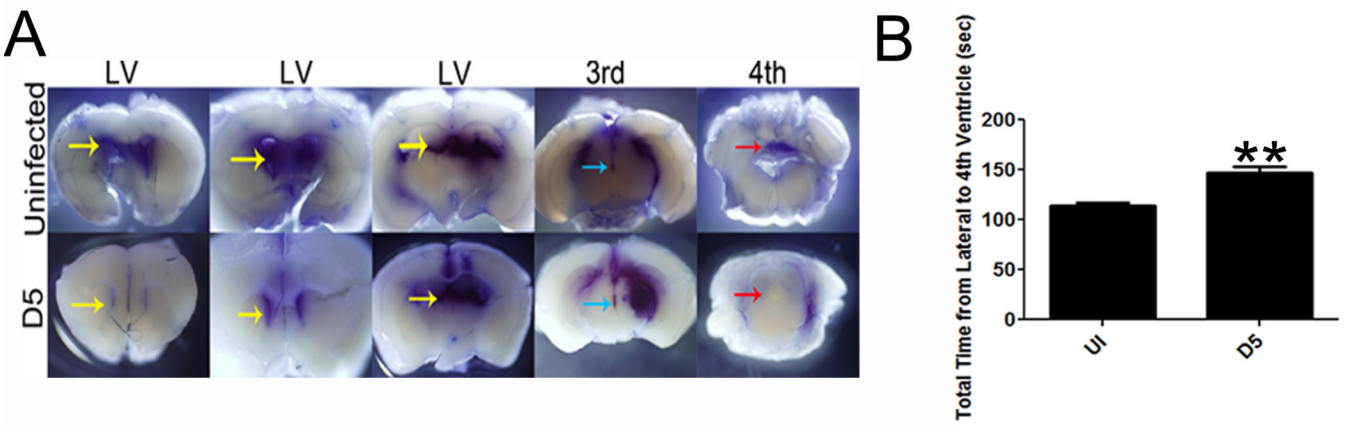

Figure 6.

CSF is blocked from draining in the ventricle of HSE CD118$^{-/-}$ mice. CD118$^{-/-}$ mice were infected with 1,000 PFU / eye HSV-1. Five days pi, the stereotactic placement of Evan's blue dye was administered into the lateral ventricles. (**A**) Tissue was then fixed and imaged for Evan's blue dye. (**B**) The time it took the dye to travel from the lateral ventricle to the 4th ventricle was recorded and compared to uninfected controls. Results and images are representative of 2 independent experiments of 3–4 mice / group. Yellow arrows, lateral ventricle; blue arrow, 3rd ventricle; red arrow, 4th ventricle; ** $p<0.01$, comparing the encephalitic to uninfected animals.

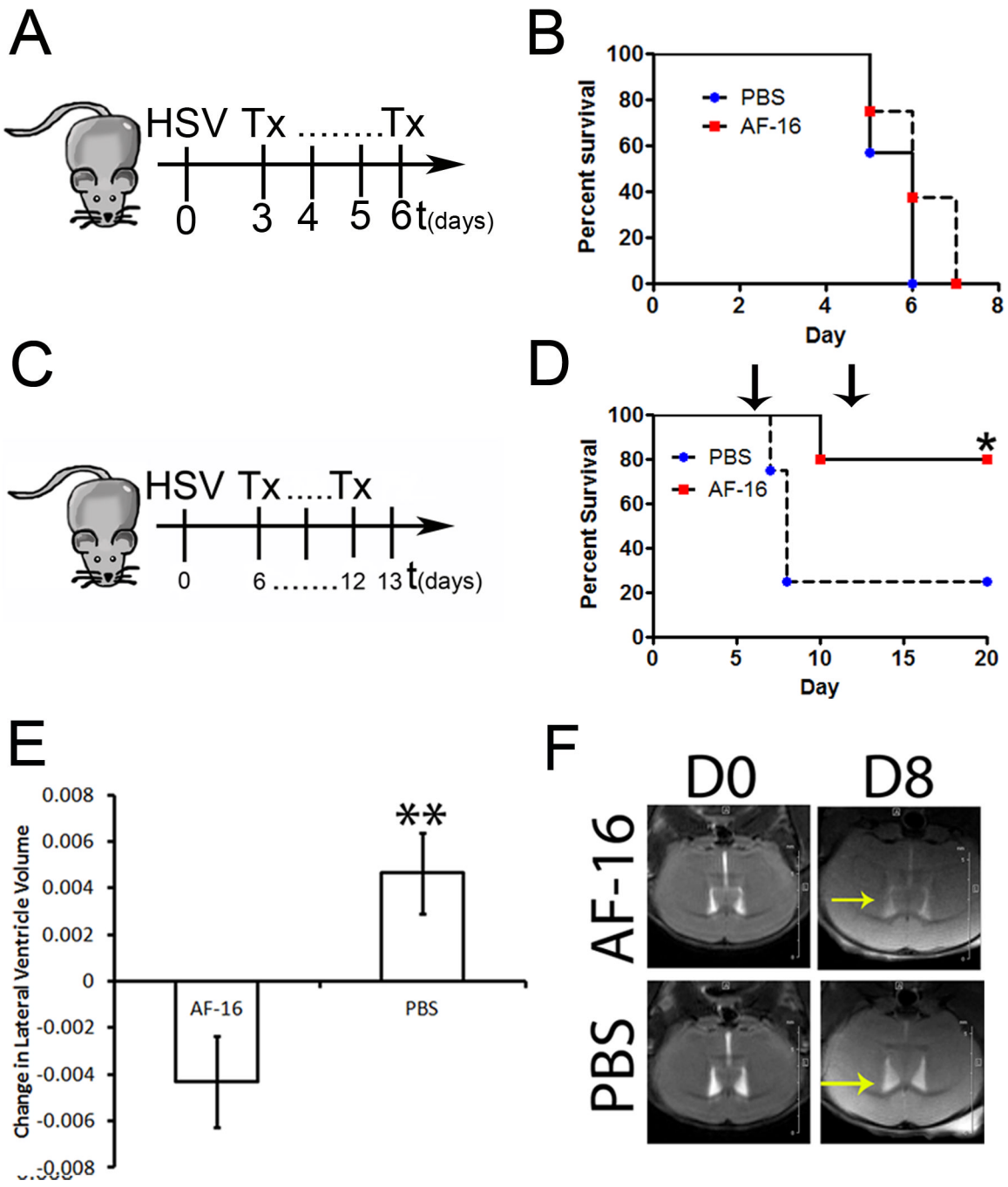

Figure 7.

A reduction in lateral ventricle enlargement attenuates disease course in CD118$^{-/-}$ mice and significantly improves survival in WT mice infected with HSV-1. (**A**) To evaluate the effect increased CSF pressure had on mouse survival, highly susceptible CD118$^{-/-}$ mice were infected and then treated 3 days pi with an intranasal dose of PBS or AF-16 twice daily. (**B**) CD118$^{-/-}$ mice treated with AF-16 on average lived longer than PBS treated controls. Results are representative of 2 independent experiments of a total of 7–8 mice / group. (**C–F**) WT mice were infected with 10,000 PFU / eye HSV-1 and were then treated twice-a-day with AF-16 or PBS starting on day 6 pi until day 12 pi (indicated by black arrows). Survival

(**D**) and lateral ventricle volume at day 8 (**E**) were then assessed. The graph represents 2 experiments of 2–3 mice / group/experiment. (**F**) Representative MRI scans at day 0 and day 8 pi and is expressed as mean change in volume ± SEM (yellow arrows, lateral ventricles). **p< 0.01; *p < 0.05 comparing peptide- to vehicle-treated groups.

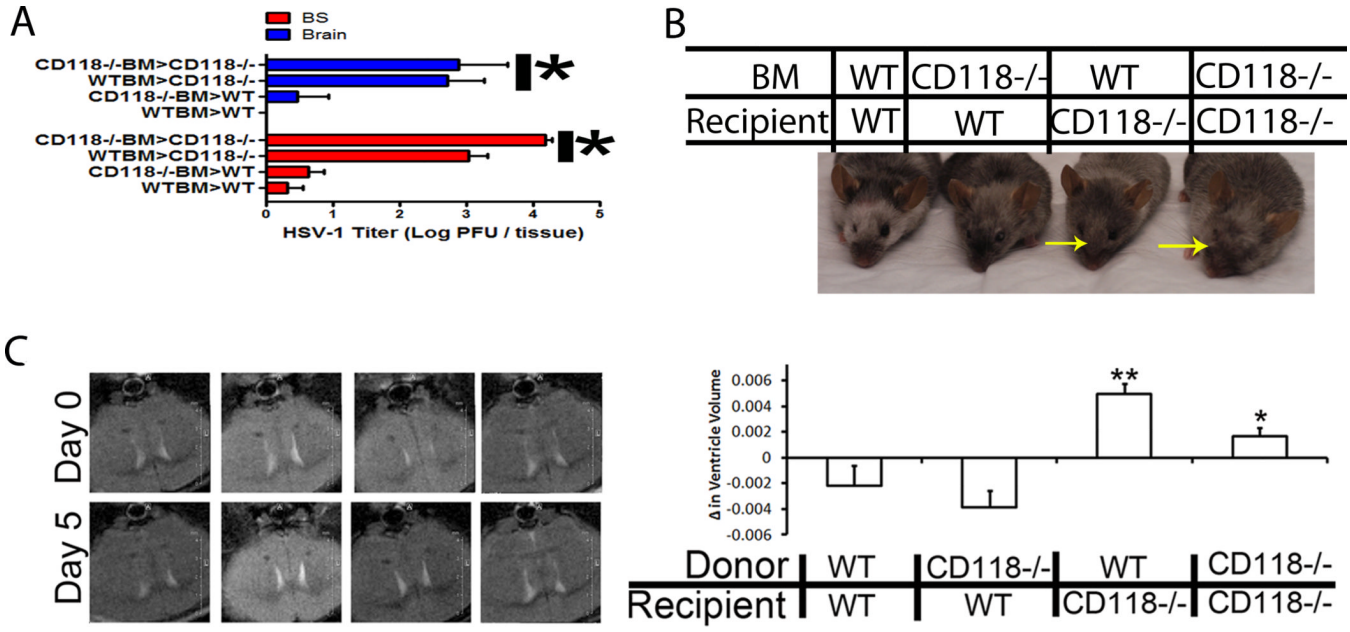

Figure 8.

Loss of resident protection results in ventricular enlargement. To identify the cell responsible for viral containment in the CNS, a chimeric mouse model using WT and CD118$^{-/-}$ mice. Mice were infected with 1,000 PFU/cornea of HSV-1 and euthanized 5 days pi. (**A**) Tissue obtained from the brain stem (BS) and brain cortex (brain) were collected and processed for viral titer by plaque assay. Results are presented as the mean log PFU HSV-1/ tissue ± SEM; n = 5–12 / group from two independent experiments. It should be noted the resident population afforded CNS protection from HSV-1 with greater than a 2 log reduction in HSV-1 recovered regardless of the source of bone marrow cells. (**B**) Irradiated WT mice given WT or CD118$^{-/-}$ BM were resistant to head swelling observed in irradiated CD118$^{-/-}$ mice given WT or CD118$^{-/-}$ BM. Yellow arrows indicate significant head swelling. (**C**) CD118$^{-/-}$ and WT mouse chimeras were imaged by T2-weighted imaging for ventricle enlargement following infection. By day 5 pi, CD118$^{-/-}$ mouse recipients of WT or CD118$^{-/-}$ bone marrow had significantly larger lateral ventricles compared to WT recipient chimeras. Results represent 3 independent experiments of 1 mouse / group/expt. **p<0.01, *p<0.05 comparing WT recipient to CD118$^{-/-}$ recipient mouse chimeras.

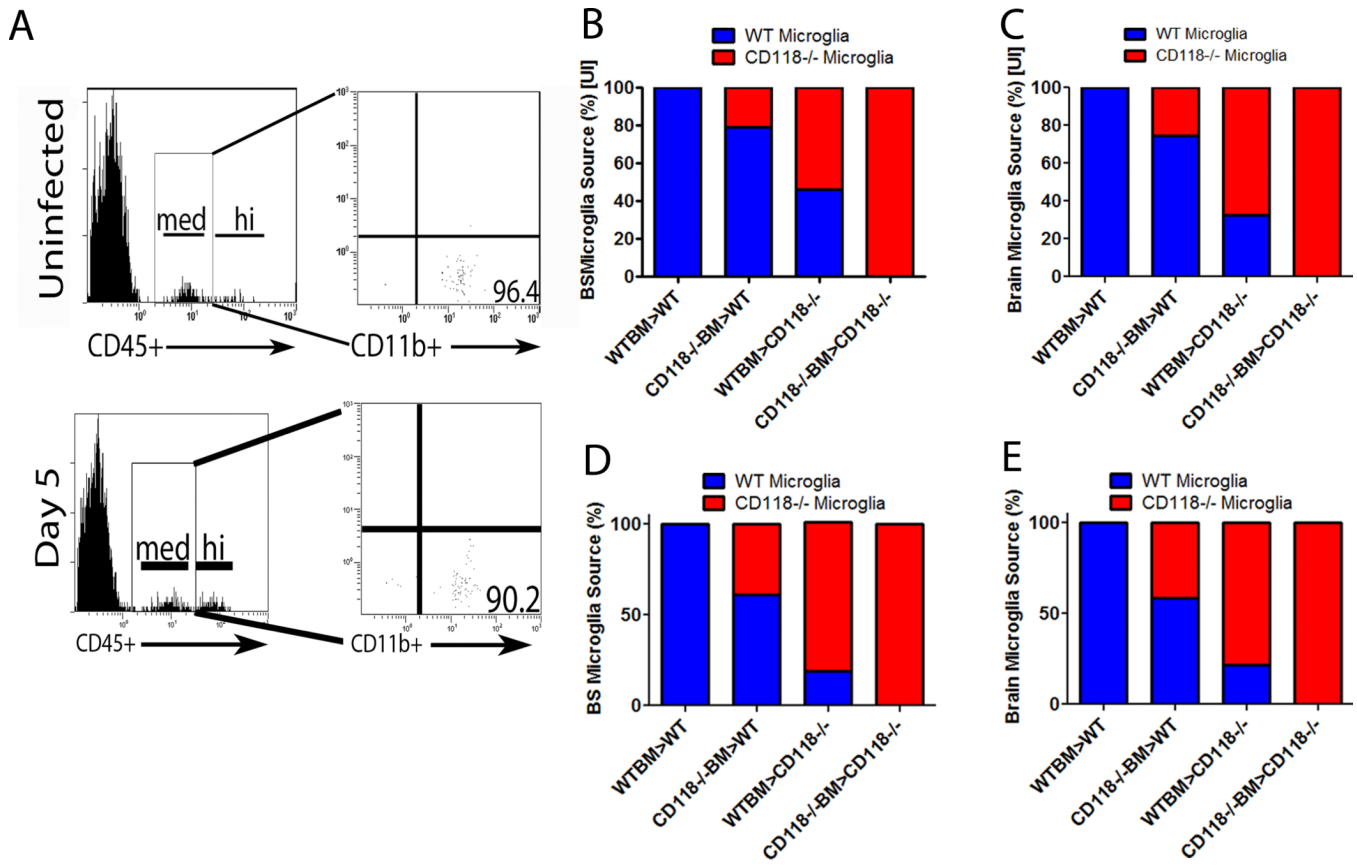

Figure 9.

The irradiated mouse chimera is the major source of microglia in the CNS. CD118$^{-/-}$ and WT mouse chimeras were established and (**A**) CD45^{med} –gated cells obtained from single cell suspensions of mouse brain were stained for CD11b and analyzed by flow cytometry. Greater than 90% from infected and 95% from uninfected mice of gated cells stained positive for CD11b confirming a microglia cell population. (**B–E**) The source of microglia was linked to the resident population in uninfected (**B, C**) and infected (**D, E**) mouse chimeras in the BS (**B, D**) and brain (**C, E**) using CD45.1 and CD45.2 gating. Histograms are representative of 3 independent experiments, n=2/group/experiment.

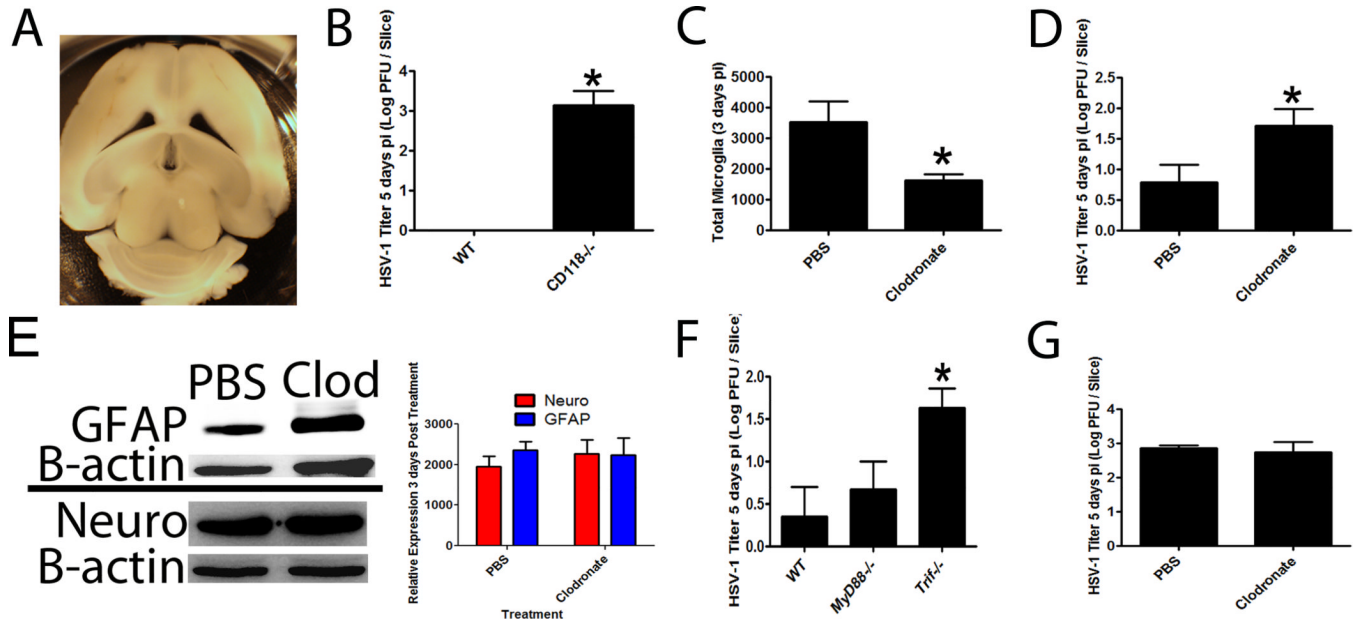

Figure 10.

TLR-3 driven microglia responses prohibit HSV spread. (**A**) A brain slice organotypic culture system was developed, and tissue slices were viable for at least 7 days as evident by conversion of Presto blue^{tm} substrate to red (data not shown). Images are representative of 2 independent experiments. (**B**) WT and CD118$^{-/-}$ brain slices were infected with 1,000 PFU / slice to confirm susceptibility of CD118$^{-/-}$ tissue. Results are a summary of 2 independent experiments of 3–4 slices / group. *p<.05 comparing CD118$^{-/-}$ to WT group. (**C**) WT tissue was subjected to specific depletion of microglia with clodronate liposomes resulted in a significant reduction in CD45^{med}CD11b^{+} cells. *p<.05 comparing PBS-liposome to clodronate-liposome treated organotypic cultures (n=6–8 slices/group). (**D**) The infection of microglia-depleted organotypic brain slice cultures with 10,000 PFU / slice resulted in significantly (*p<.05) higher viral titers (n = 6–8 slices / group). (**E**) Clodronate liposome and PBS liposome treated cultures were assessed for astrocyte (GFAP) and neurons (Neuro) by Western blot analysis. A representative blot (taken from two experiments) is shown in the left panel with the summary densitometric analysis shown on the right panel. (**F**) To identify the critical innate sensor within the CNS, WT, MyD88$^{-/-}$ and Trif$^{-/-}$ organotypic brain slice cultures were infected with 10,000 PFU / slice and viral content evaluated 5 days pi. Results are a summary of 2 independent experiments (n=2–3/group/experiment), *p<.05 comparing the TRIF$^{-/-}$ to WT and MyD88$^{-/-}$ brain slice groups. (**G**) Clodronate or PBS liposome-treated brain slice cultures from TRIF$^{-/-}$ mice were infected as in (F) and viral content evaluated 5 days pi. Results are a summary of 2 independent experiments (n=2–3/group/experiment) and expressed as mean log PFU HSV-1/slice.